16A.3 OPERATIONAL IMPLICATIONS FOR NEXRAD WSR-88D WIND SPEED REDUCTION FACTORS

Richard J. Krupar III* and John L. Schroeder
National Wind Institute, Texas Tech University, Lubbock, Texas

1. INTRODUCTION

The ratio of the gust or mean surface-level wind speed to the gradient wind speed is known as the wind speed reduction factor (WSRF). The WSRF is commonly used to determine both peak and mean surface-level wind speeds both over water and land. Wind engineers and meteorologists typically use flight-level aircraft, Stepped Frequency Microwave Radiometer (SFMR), and Global Positioning System (GPS) dropwindsonde wind measurements to determine over water WSRFs (Franklin et al. 2003; Powell et al. 2009), while radiosonde and Doppler radar wind measurements have been used to compute WSRFs overland (Sparks and Huang 2001).

Historical overland WSRF studies were summarized by Vickery et al. (2009). The authors state that Schwerdt et al. (1979) computed a coastal WSRF of 0.845 and an overland WSRF of 0.745 (19 km inland of the coast), while Batts et al. (1980) and Georgiou et al. (1985) computed overland WSRFs of 0.740 and 0.620 respectively. With regard to the underlying terrain conditions dictating the overland WSRFs, Vickery et al. (2009) express that Schwerdt et al. (1979) stated that the roughness regime was not rough, Batts et al. (1980) assigned a value of 0.005 m to the terrain, and Georgiou (1985) indicated that open terrain conditions could be assumed. Sparks and Huang (2001) computed WSRFs over land using radiosondes, Doppler radar, and automated surface observing system (ASOS) wind measurements taken at 10 m height above ground level (AGL) for four hurricanes. Comparisons with ASOS wind measurements were restricted to locations within 25 km of sites where the gradient wind speed was calculated and when wind speeds were not variable over a short period of time. Moreover, hourly mean wind speeds centered on the gradient wind speed determination were restricted to values stronger than 15 m s^{-1} and peak 5-second gusts measured during the hour to values greater than 20 m s^{-1}. This study found that in the absence of convection, on average, the hourly mean wind speed is approximately 44% of the gradient wind speed and the peak 5-second gust measured during the hour is 1.57 times the hourly mean wind speed. Open terrain conditions were implied.

Historical ASOS and Texas Tech University Hurricane Research Team (TTUHRT) wind measurements have been gathered along with Velocity Azimuth Display (VAD) wind profiles generated from coastal NEXRAD WSR-88D radars to compute overland WSRFs. The WSRFs were analyzed in a storm-relative framework to examine storm-to-storm dependencies. The goal of the study is to determine whether or not an empirical relationship can be formulated for overland WSRFs using VAD Doppler radar wind measurements and both existing and historical surface-level wind measurements.

2. DATA AND METHODOLOGY

ASOS 1-minute data were retrieved from the National Climatic Data Center (NCDC). The 2-minute mean wind speed reported every minute is calculated by averaging all of the 5-second averages over the previous 2-minute period. The peak 5-second gust is taken as the maximum 5-second average measured during the previous minute. Standard measurement height is 10 m AGL, however, not all ASOS sites abide by the standard. Historical TTUHRT wind measurements are composed of StickNet measurements that sample at 1, 5, and 10 Hz at a measurement height of approximately 2.25 m. Surface-level wind speed data are selected based on the distance criteria proposed by Sparks and Huang (2001).

The mean boundary layer wind (MBLW) is determined from VAD wind profiles and is used to represent the source of momentum available for transport to the surface. Powell et al. (2003) indicated that the gradient wind speed is difficult to assign to hurricanes because gradient balance may extend to heights as high as 3 km AGL. Also, the authors suggest that the lack of an objective

* *Corresponding author address*: Richard J. Krupar III, National Wind Institute, Texas Tech Univ., Lubbock, Texas 79409-3155; e-mail: richard.krupar@ttu.edu.

approach to determine the hurricane boundary layer (HBL) height, inflow depth, gradient wind speed, and maximum wind speed height makes it difficult to scale wind speeds and heights properly.

The representative averaging time of the VAD wind profile is difficult to assign given that the measurement is averaged spatially and temporally. The VAD measurement is representative of the time it takes to complete a volume coverage pattern (VCP) above the radar. For the purpose of this study, the averaging time of the VAD wind measurement is disregarded. To align both the surface tower and VAD MBLW speed measurements, an hour moving average was passed over both the surface tower and VAD wind profile data and was centered on the radar time stamp representative of the middle of the VCP employed. Hurricanes that come within 150 km of coastal NEXRAD WSR-88D sites were selected for comparison. Table 1 lists all of the comparisons used in this study.

Table1. A list of Doppler radars, surface towers, storms, and the distance between the radar sites and surface towers.

Radar ID	Surface Tower ID	Storm Name	Year	Distance (km)
KBRO	KBRO	Emily	2005	00.42
KBRO	KBRO	Dolly	2008	00.42
KBRO	SN0102B	Dolly	2008	23.24
KBRO	SN0214B	Dolly	2008	04.01
KBRO	SN0216B	Dolly	2008	13.26
KBRO	SN0218B	Dolly	2008	20.88
KBRO	SN0222B	Dolly	2008	13.56
KAMX	KMIA	Katrina	2005	21.52
KAMX	KMIA	Wilma	2005	21.52
KAMX	KTMB	Wilma	2005	04.00
KMOB	KMOB	Katrina	2005	01.12
KBYX	KEYW	Katrina	2005	06.51
KBYX	KEYW	Charley	2004	06.51
KJAX	KJAX	Fay	2008	01.40

Surface tower measurements below 10 m were adjusted to 10 m using the following neutral stability similarity relationship:

$$\frac{U_{10}}{U_Z} = \frac{\ln(\frac{10 - Z_D}{Z_0})}{\ln(\frac{Z - Z_D}{Z_o})} \qquad (1)$$

where U_Z is the mean wind speed at height Z, Z_D is the zero-plane displacement height (assumed to be zero for the purpose of this study), U_{10} is the 10 m mean wind speed, and Z_o is the roughness length. Values of Z_o were computed in different manners depending on the surface measurement platform. For ASOS platforms, 45º degree sector mean Z_o values were obtained from Dr. Frank Lombardo's ASOS Z_o database, and used to standardize 10 m mean wind speeds to open exposure (Z_o = 0.03 m). For StickNet platforms, a ten minute moving average was passed over the raw 2.25 m wind speed data and the TI method outlined by Beljaars (1987) was used to compute values of Z_o. Then, 30º degree sector mean Z_o values were computed. Equation 1 was used to adjust the measurement height to 10 m AGL and the friction velocity/roughness length relationship proposed by Simiu and Scanlan (1996) was employed to the 10 m wind measurement to adjust the reference exposure to open exposure.

All 10 m mean wind speeds less than 8 m s^{-1} wind speed were thrown out initially. Thresholded mean wind speeds were then divided by the corresponding VAD MBLW speed to obtain WSRFs. The WSRFs were binned by normalized distance (radius/radius of maximum wind) from surface tower to storm center using 1 radius resolution bins ranging from 0-10 radii from storm center. Mean and median WSRFs for each normalized distance bin were computed and normalized distance-dependent WSRF curves were generated for each storm and radar site.

3. Results

Wind speed reduction factors were computed for each of the radar-surface tower comparisons listed in Table 1. Comparisons were made between individual storms at one radar site, as well as, across all radar sites. Additionally, normalized distance-dependent WSRFs were used to adjust MBLW speeds to the 10 m observation height and were compared with individual storm normalized distance-dependent WSRFs, where there were normalized distance bins that overlapped. The mean and median WSRFs for each storm were also compared at each site, as well as, the WSRF associated with the maximum surface mean wind speed.
A histogram of 3,103 WSRFs generated from ASOS, StickNet, and NEXRAD WSR-88D wind data in Table 1 is displayed in Figure 1. The WSRFs follow a lognormal distribution. This observation is shown in Figure 2. The mean and standard deviation of the lognormal distribution displayed in Figure 2 is 0.6236 and 0.0122 respectively.

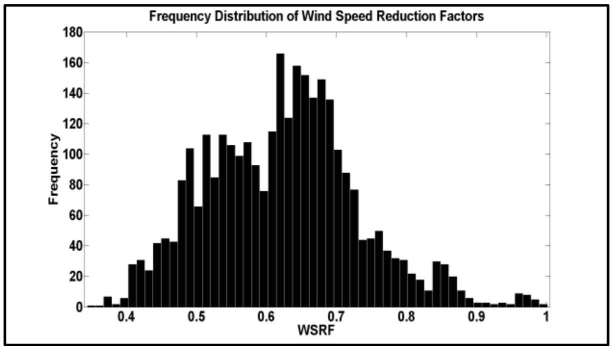

Figure 1. Histogram of all contributing wind speed reduction factors.

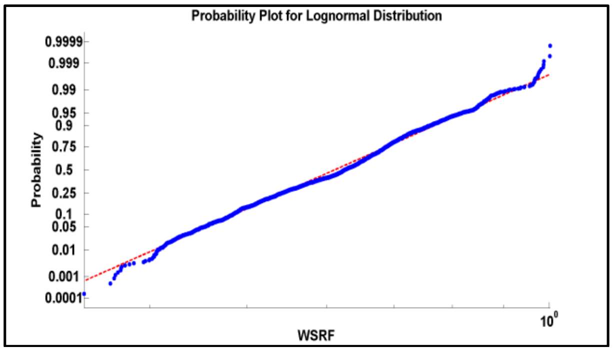

Figure 2. Probability plot comparing lognormal distribution to the distribution of the wind speed reduction factors.

Figure 3 shows all of the WSRFs computed using 10 m, open exposure surface wind measurements surrounding the Brownsville, Texas NEXRAD WSR-88D radar (KBRO) during Hurricanes Emily (2005) and Dolly (2008) and the MBLW derived from VAD wind profiles taken at KBRO. A total of 1,578 WSRFs were computed and distances from surface measurement sites to storm centers were normalized by the storm-relative radius of maximum wind (RMW) interpolated from H*Wind. As can be seen from Figure 3, no evident relationship appears to exist between the WSRFs and normalized radii. Surface roughness influences have been removed by standardizing the measurement height and exposure, however, other influences such as variable MBLW speeds and storm-relative position may be influencing the variability noted.

Figure 4 displays the median normalized distance-dependent WSRF curves generated for Hurricanes Katrina (2005) and Wilma (2005) using ASOS wind data from KMIA and KTMB and NEXRAD WSR-88D VAD wind profiles from Miami, Florida (KAMX). It can be seen in Figure 4 that each ASOS WSRF curve does not overlap between 0-7 radii from storm center. The lack of overlapping samples results in an incomplete picture of how the WSRFs vary over the entire range of normalized radii between the two storms.

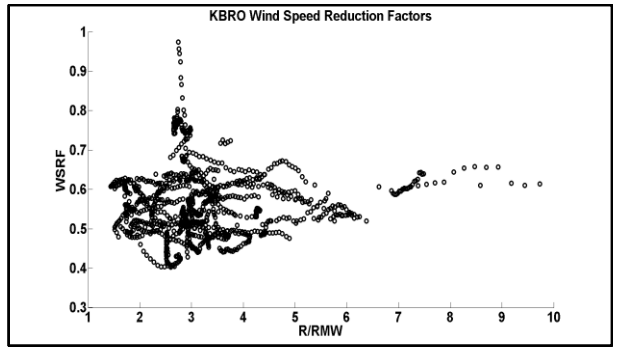

Figure 3. Wind speed reduction factor versus normalized radius from KBRO during Hurricanes Emily and Dolly.

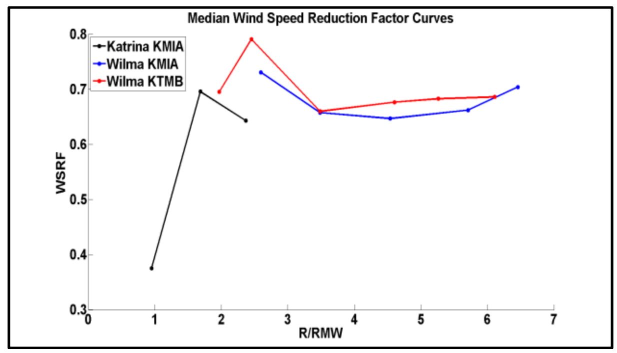

Figure 4. Comparison of median wind speed reduction factor curves versus normalized radii.

Despite the lack of overlapping samples in Figure 4, the KMIA and KTMB WSRF curves are still closely spaced together.

Figures 5-6 show the 10 m, open exposure mean wind speeds collected during Hurricanes Katrina (2005) and Wilma (2005) at KMIA, as well as, the adjusted KAMX MBLW speed using the KAMX site-specific median and mean WSRF curves. The median normalized distance-dependent WSRF curve for KAMX underestimates the KMIA mean wind speed in Figure 5 up to approximately radar volume 100 and then overestimates the eye and eyewall wind speeds as Hurricane Katrina continues propagating west-southwest to southwest. The median normalized distance-dependent WSRF curve performs better for the Hurricane Wilma KAMX-KMIA comparison (Figure 6), however, the KAMX site-specific WSRF curve overestimates the Wilma (2005) KMIA mean wind speed around radar volume 50 and underestimates the mean wind speed beyond radar volume 85.

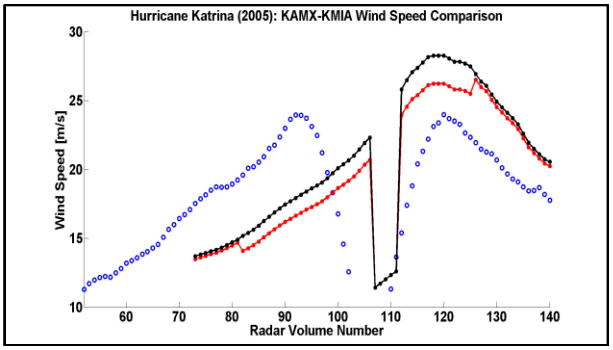

Figure 5. Comparison of KMIA mean wind speed (blue circles) with median (red) and mean (black) adjusted KAMX MBLW speed.

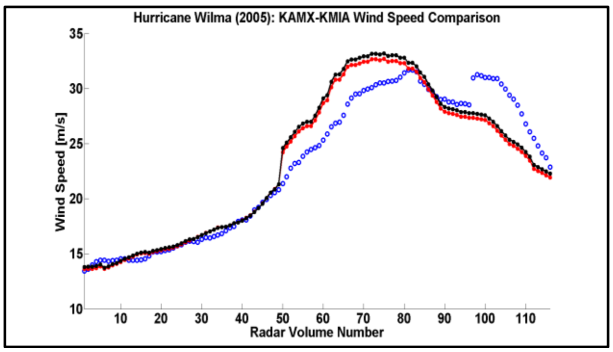

Figure 6. Comparison of KMIA mean wind speed (blue circles) with median (red) and mean (black) adjusted KAMX MBLW speed.

A similar comparison was made with the same sites but instead the mean normalized distance-dependent WSRF curve was used to adjust the KAMX MBLW speeds to 10 m height AGL. Figures 5-6 indicate that the KMIA site-specific curve behaves no better than the median WSRF curve employed. It is believed that both the median and mean normalized distance-dependent WSRF curves fail to reproduce the shape of the ASOS mean wind speed time series because of a lack of data within each of the normalized distance bins. Additionally, storm-relative position, as well as, MBLW speed variability associated with hurricane dynamics may be inducing differences within similar normalized distance bins. Sharp changes in wind speed and/or direction may also be impacting the poor alignment between the original and adjusted 10 m mean wind speeds (Sparks and Huang 2001).

The final assessment conducted in this study involved computing single mean and median WSRFs for the duration of time when the one hour MBLW speed exceeded 30 m s^{-1} over the KBRO NEXRAD WSR-88D radar site during Hurricane Dolly (2008). Also, the WSRF associated with the maximum one hour mean wind speed at 10 m AGL was used for comparison. Figure 7 compares the use of the mean, median, and site-specific surface maximum WSRFs to adjust MBLW speeds during Hurricane Dolly (2008) at the nearest ASOS (KBRO). As can be seen in Figure 7, the mean and median WSRFs performed better on the whole than the maximum WSRF. However, it is evident that the entire 10 m ASOS mean wind speed time history cannot be reproduced simply by applying a single WSRF to the MBLW wind speed. Moreover, the maximum WSRF barely estimates the maximum 10 m ASOS mean wind speed and overestimates the rest of the time history.

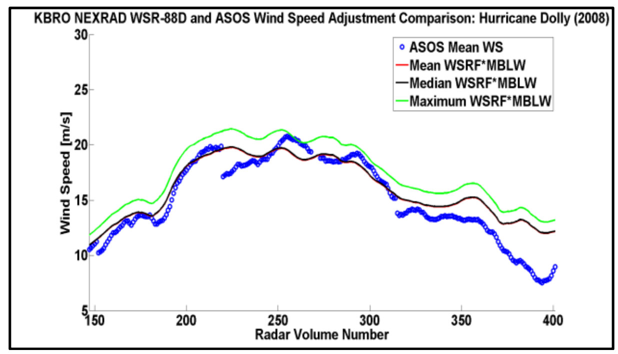

Figure 7. Comparison of single wind speed reduction factor adjustments to the MBLW speed with the KBRO ASOS mean wind speed.

Table 2 lists the mean, median, and site-relative maximum WSRFs for each of the radar-tower comparisons made during Hurricane Dolly (2008). MBLW speeds above 30 m s^{-1} and attendant 10 m surface wind speeds are only used to compute the WSRF summary statistics. Additionally, the normalized radius at the time of the site-relative maximum WSRF is also shown in Table 2. The mean WSRFs range from 0.4860-0.5989, while the median WSRFs range from 0.4807-0.5961. Larger variability is noted in the site-relative maximum WSRFs, where SN0216B produced the largest site-relative maximum WSRF (0.9740). The large difference between SN0216B and the rest of the surface towers is likely a result of the standardization process. SN0102B had the lowest mean and median WSRFs and is the farthest probe away from the KBRO NEXRAD WSR-88D radar. SN0214B had the largest normalized distance from measurement site to storm center but still exceeded the mean and median WSRFs of SN0102B. None of the statistics account for storm-relative position or distance from measurement site to storm center, which is believed to be responsible for some of the variability noted.

Table 2. Wind speed reduction factor summary statistics for all surface tower measurement collected during Hurricane Dolly (2008).

Tower ID	Mean	Median	Max	R/RM W
KBRO	0.5832	0.5847	0.6327	2.8554
SN0102B	0.4860	0.4807	0.6215	1.7057
SN0214B	0.5166	0.5150	0.5516	4.2603
SN0216B	0.5989	0.5611	0.9239	2.7852
SN0218B	0.5576	0.5961	0.6382	2.5436
SN0222B	0.5524	0.5594	0.6734	2.8789

4. Summary

Historical surface wind data and NEXRAD WSR-88D VAD wind speed profiles were gathered and used to generate one hour mean WSRFs. Surface wind measurements not originally collected at 10 m were adjusted from their reference height to 10 m and standardized to open exposure to remove the influence of variable surface roughness. WSRFs were further segregated into normalized distance bins to examine the dependence of normalized distance from surface measurement site to storm center on the WSRFs. No clear relationship exists between the normalized radii and WSRFs. Future work will further segregate the WSRFs into MBLW speed groups and storm-relative position (i.e. right and left of storm track).

Storm and NEXRAD WSR-88D radar site-specific WSRF curves were created and compared. Results from the comparisons indicate that not enough observations exist at some sites to fully determine a radar-site specific WSRF curve. Adjustments to the MBLW speeds using the radar site-specific curves revealed that storm differences influence the final adjustment. This approach was determined to be more objective than simply applying one mean, median, or site-specific maximum WSRF since not enough variability is explained by the single WSRF statistic. Future work will examine different VAD layer average wind speeds, as well as, how the height of the maximum wind speed contained in the VAD wind profile varies and influences the WSRF. Additionally, surface gust-to-gradient WSRFs will be generated and assessed in a similar manner to the one hour mean WSRFs.

5. References

Beljaars, A. C. M., 1987: The measurement of gustiness at routine wind stations – a Review. Scientific Report WR87-11, KNMI, de Bilt, Netherlands, 1–50.

Franklin J. L., M. L. Black and K. Valde, 2003: GPS dropwindsonde wind profiles in hurricanes and their operational implications. *Wea. Forecasting*, **18**, 32–44.

Powell M. D., P. J. Vickery and T. A. Reinhold, 2003: Reduced drag coefficient for high wind speeds in tropical cyclones. *Nature*, **422**, 279-283.

Powell M. D., E. W. Uhlhorn and J. D. Kepert, 2009: Estimating maximum surface winds from hurricane reconnaissance measurements. *Wea. Forecasting*, **24**, 868-883.

Simiu, E. and R.H. Scanlan, 1996: *Wind Effects of Structures: Fundamentals and Applications to Design*. Wiley, 589 pp.

Sparks P. R. and Z. Huang, 2001: Gust factors and surface-to-gradient wind-speed ratios in tropical cyclones. *J.Wind Eng. Ind. Aerodyn.*, **89**, 1047-1058.

Vickery P. J., F. J. Masters, M. D. Powell, and D. Wadhera, 2009: Hurricane hazard modeling: The past, present, and future. *J.Wind Eng. Ind. Aerodyn.*, **97**, 392-405.